Pergamon

Pattern Recognition, Vol. 30, No. 9, pp. 1387–1400, 1997

0031-3203/97 $17.00+.00

PII: S0031-3203(96)00180-X

DETERMINATION OF FEATURE CORRESPONDENCES IN STEREO IMAGES USING A CALIBRATION POLYGON

JUI-MAN CHIU,[†] ZEN CHEN,[†,*] JEN-HUI CHUANG[‡] and TSORNG-LIN CHIA[§]

[†]Institute of Computer Science and Information Engineering, National Chiao Tung University, Hsinchu, Taiwan, R.O.C.

[‡]Institute of Computer and Information Science, National Chiao Tung University, Hsinchu, Taiwan, R.O.C.

[§]Department of Electrical Engineering, Chung Cheng Institute of Science and Technology, Tao-Yuan, Taiwan, R.O.C.

(*Received* 16 *April* 1996; *in revised form* 24 *October* 1996; *received for publication* 4 *November* 1996)

Abstract—In this paper, we propose a novel approach to solving the vertex/edge correspondence problem for stereo images. Assume an object is placed on a calibration plate (C-plate) and two perspective views of them are given. The C-plate vertex correspondence, determined by cross-ratios, is used to reduce the search space for determining object vertex/edge correspondence. First, the correspondence of object edges lying on the C-plate (called the object base edges) is considered. This is because the subpolygons obtained from the division of the C-plate by the extended line of each of these base edges are viewpoint invariant, i.e. the cross-ratio of each of their vertices in different images will have equal value. Assume that at least one of the base edges is visible in each image. Since a visible object base edge has to be an object boundary edge in an image, only object boundary edges will be considered for the cross-ratios check for the associated subpolygons as well as other geometric constraint checks in determining the object base vertex/edge correspondence. These geometric constraints include (i) the position of the edges along the boundary of object faces, and (ii) the division of the C-plate vertices by the extended lines of these edges. Based on one of the determined corresponding base edge pairs, the correspondence of all other edges can be determined by constraints similar to (i). Finally, some additional viewpoint invariant measures about the object faces and the C-plates are introduced to resolve the ambiguity problem which may arise for specific viewpoints and some special object shapes. The proposed approach only needs 2-D image data and has no constraint on the number of vertices of an object face. Experimental results are presented for some polyhedral as well as curved objects. © 1997 Pattern Recognition Society. Published by Elsevier Science Ltd.

Stereo vision Feature correspondence Calibration plate Viewpoint invariant Cross-ratio

1. INTRODUCTION

In stereo vision, reconstructing the 3-D information of an object requires finding feature correspondence from two perspective views of the object. Techniques for solving the correspondence problem can be divided into two categories:[1,2] area-based stereo techniques and feature-based stereo techniques. Since area-based stereo techniques are sensitive to the change of the perspective distortions and intensity, and are slower, most researchers use the feature-based stereo techniques,[3–13] which choose image features such as corner points, junctions, line segments, etc., as primitives for correspondence matching. Most feature-based stereo techniques employ an epipolar line approach,[3–11] such that a designated feature in one image is matched with features on the epipolar line in the other image. Since other 3-D feature points on the epipolar plane will also be projected onto the epipolar line, often more than one feature appears on the epipolar line. In such a circumstance, one cannot be sure of the feature of the true correspondence without additional information, i.e. an ambiguity problem arises. Many researchers try to use disparities of features,[3,4] geometric constraints,[5–9] the intensity of neighborhoods,[10,11] or some other heuristics to resolve the problem, but still cannot avoid the ambiguities completely. Although the epipolar line approach searches corresponding features in a 2-D image, the approach needs to use the 3-D information of two camera lens centers to construct an epipolar plane before building the epipolar line of each feature and is thus inefficient.

Lei[14] presents a method to match planar polygons of more than four vertices in two images using the cross-ratios. It is shown that the value of the cross-ratio of each of the vertices is viewpoint invariant. Since the method does not use 3-D information, it is simple. The method can be used to match polyhedral objects with the requirement that at least one of the polyhedral faces have more than four vertices. For every possible pair of corresponding polyhedral faces from two images, the method must compute and cyclically match the cross-ratios for every vertex. Therefore, it requires much computation time and matching frequency.

In this paper, we propose a novel approach to solving the vertex/edge correspondence in the stereo images. The

* Author to whom correspondence should be addressed. E-mail: zchen@csie.nctu.edu.tw.

images are obtained with an auxiliary planar calibration plate (C-plate) placed under the object. It is shown that with the extra information provided by the C-plate, the following objectives can be attained:

1. The number of vertices of each object face can be less than five.
2. Only the 2-D image data is needed for determining the vertex/edge correspondence.
3. The exhaustive search for cyclically matched cross-ratio sequences for the vertices of each of the feasible object face pairs can be avoided.
4. The ambiguity in the feature correspondence can be resolved for general situations.

According to the proposed approach, the C-plate vertex correspondence is first determined using cross-ratios; the result is then used to reduce the search space for determining object vertex/edge correspondence. First, the correspondence of object edges lying on the C-plate (called the object base edges) is considered. This is because the subpolygons obtained from the division of the C-plate by the extended line of each of these base edges are viewpoint invariant, i.e. the cross-ratio of each of their vertices in different images will have equal value. Since a visible object base edge must be an object boundary edge in an image, only object boundary edges will be considered for determining the object base vertex/edge correspondence. The correspondence is determined by cross-ratios check for the associated subpolygons as well as other geometric constraint checks about the boundary edges. These geometric constraints include (i) the position of the edges along the boundary of object faces, and (ii) the division of the C-plate vertices by the extended lines of these edges. Based on one of the determined corresponding base edge pairs, the correspondence of all other edges, including the non-base edges, can be determined by constraints similar to (i). Finally, some additional viewpoint invariant measures about the object faces and the C-plates are introduced to resolve the ambiguity problem which may arise for specific viewpoints and some special object shapes.

The remainder of this paper is organized as follows. Section 2 describes the method of finding possible base vertex/edge correspondence based on viewpoint invariant features in two images. The efficiency of the proposed four-step procedure is achieved by using the predetermined C-plate vertex correspondence. Based on one of the determined corresponding base edge pairs, Section 3 describes the procedure for determining the correspondence of other edges. The possibilities of using other viewpoint invariant measure to resolve the ambiguity problems that arise for specific viewpoints and some special object shapes are also presented. Section 4 presents an extension of the proposed approach when the C-plate boundary is partially occluded. Section 5 illustrates the implementation of our method and presents some experimental results. Some concluding remarks are given in Section 6.

2. FINDING POSSIBLE BASE VERTEX/EDGE CORRESPONDENCES BASED ON VIEWPOINT INVARIANT FEATURES IN TWO IMAGES

Assume that an object is placed on the C-plate and the boundary of the C-plate is not occluded by the object. The extended line of a base edge of the object will divide the C-plate into two subpolygons which are invariant with respect to different viewpoints. The main idea of the proposed approach is to use the viewpoint invariant property of the subpolygons to find the possible base vertex/edge correspondence.

It is obvious that any visible object base edge has to be a boundary edge of the object in an image. Thus, only these boundary edges will need to be considered in the determination of base vertex/edge correspondence. For example, Fig. 1 shows two images of a polyhedron placed on the C-plate. For the extracted object edges shown in Fig. 2, the boundary edges, represented in vertex pairs, include (0,1), (1,2), (2,3), (3,4), (4,5), (5,10), (10,9), and (9,0), while the rest are internal edges. Among these boundary edges, edges (0,1), (1,2), (2,3), and (3,4) are visible base edges. In general, the straight line containing a boundary edge can divide the C-plate into two subpolygons in the image (see Fig. 3). If the boundary edge is an image of a base edge, the associated subpolygons of the edge obtained from different viewpoints will correspond to the identical division of the C-

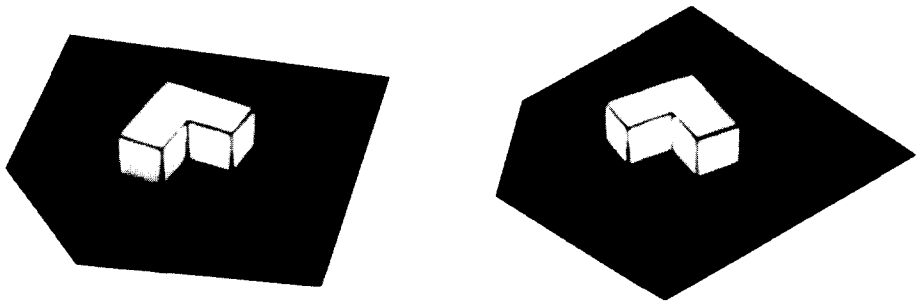

(a) (b)

Fig. 1. Two views of a polyhedron placed on the C-plate. (a) Image 1. (b) Image 2.

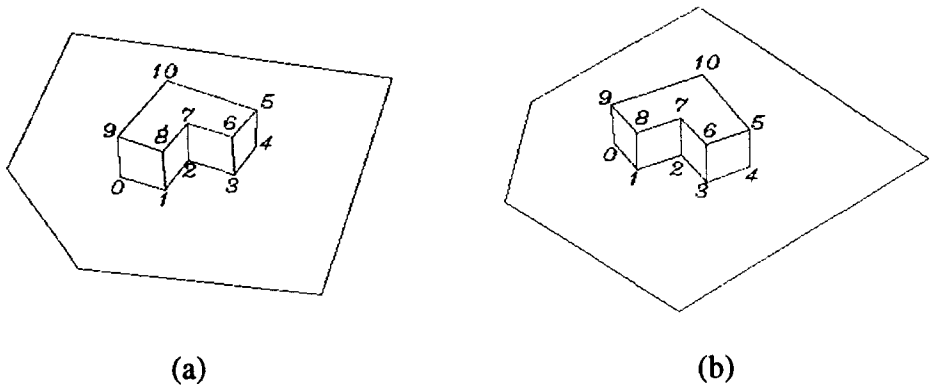

Fig. 2. Edges extracted from (a) Image 1 and (b) Image 2 of Fig. 1.

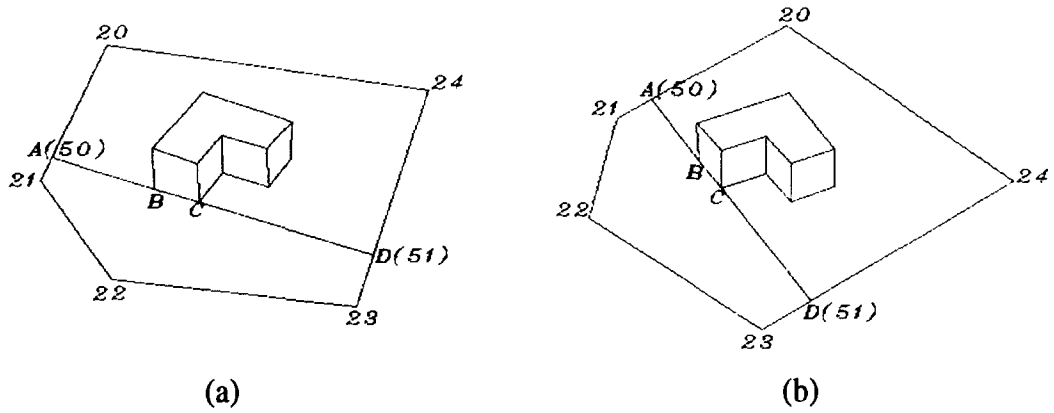

Fig. 3. Division of the C-plate into two associated subpolygons by the extended line of the object boundary edge BC in (a) Image 1 and (b) Image 2.

plate, otherwise the subpolygons will not have such a viewpoint invariant property.

According to Lei,[14] the value of the cross-ratio (which can be calculated for polygons having at least five vertices) of each of the vertices of the associated subpolygons of a base edge will be the same in images obtained from different viewpoints. Therefore, one can match the cross-ratios of the vertices of the associated subpolygons of any two boundary edges, each from a different image, to determine the possible base edge correspondence. However, the direct matching is of time complexity O(NMV), where N and M are the number of object boundary edges in Image 1 and Image 2, respectively, and V is the maximum number of vertices of the associated subpolygons containing at least five vertices. It is shown in the following that if we first determine the vertex correspondence of the C-plates in the two images by using cross-ratios, the correspondence, as an auxiliary information, can speed up the procedures for finding the base vertex/edge correspondence by reducing the search space of the matching process.

2.1. *Determination of C-plate vertex correspondences*

For determining the vertex correspondence of the C-plates in two images, it is assumed that the number of vertices of the C-plate is larger than or equal to five. Thus, the method proposed by Lei[14] can be applied. Consider the polygon shown in Fig. 4, according to Lei;[14] the cross-ratio of V_1 is viewpoint invariant and can be computed as

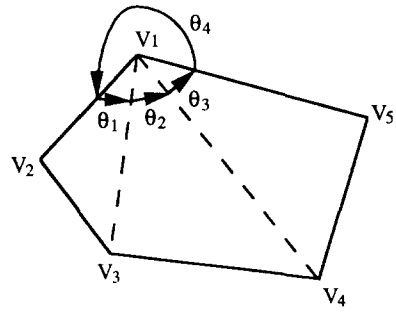

Fig. 4. Internal/external angles of a pentagon formed by $\overline{V_1V_i}$'s.

$$R_1 = \frac{\sin(\theta_1 + \theta_2)\sin(\theta_2 + \theta_3)}{\sin(\theta_2)\sin(\theta_1 + \theta_2 + \theta_3)}, \quad (1)$$

where θ_1, θ_2, and θ_3 are angles formed by the rays originating from V_1 and pointing toward its four neighboring vertices (V_2, V_3, V_4, and V_5) arranged in the counterclockwise (or clockwise) direction, with

$\sum_{i=1}^{3} \theta_i < 180°$. Let R_j^i be the cross-ratio of the jth vertex, V_j^i, of the C-plate in the ith image, $i = 1,2$; $j = 1,2,\ldots,V \geq 5$. For the vertex sequence $\{V_j^1 \mid 1 \leq j \leq V\}$, the vertex sequence $\{V_{\langle j+k \rangle}^2 \mid 1 \leq j \leq V,\ 1 \leq k \leq V-1\}$, $\langle j+k \rangle = (j+k)_{\text{mod } V}$, whose corresponding cross-ratio sequence satisfies the following criterion, is identified as the matched vertex sequence:

$$\underset{k}{\text{Min}} \sum_{j=1}^{V} |R_j^1 - R_{\langle j+k \rangle}^2|^2. \tag{2}$$

Thus, the computational complexity for determining the correspondence of C-plate vertices in two images is O(V), where V is the number of vertices of the C-plate. With the determined C-plate vertex correspondence, the object base vertex/edge correspondence can be found more efficiently, as discussed in the next section.

2.2. *Determination of object base vertex/edge correspondences*

Let $e_i^1, i = 1,2,\ldots,N$, be the ith object boundary edge in Image 1, and e_j^2, $i = 1,2,\ldots,M$, be the jth object boundary edge in Image 2. The procedure of determining if e_i^1 and e_j^2 form a corresponding base edge pair includes the four steps described next. The first two steps check if the object faces containing these edges, as well as the divisions of the C-plate by the extended lines of these edges, are geometrically consistent in the two images. The last two steps check some viewpoint invariant properties associated with the two edges.

2.2.1. Step 1: Object face vertex number check. In this step, we check if the number of vertices of the object face containing e_i^1 is identical to that for the face containing e_j^2. Given an object boundary edge in an image, the face containing the edge is unique. Such a check can prevent two boundary edges belonging to two faces containing different number of vertices, and thus corresponding to two different object edges, from being processed further in the subsequent procedure.

2.2.2. Step 2: Subpolygon's C-plate vertex check. It is easy to see that the division of the C-plate by the line containing e_i^1 is identical to that due to e_j^2 if the two edges correspond to the same object base edge. In this step, it is checked if the associated subpolygons of e_i^1 and e_j^2 have identical C-plate vertices whose correspondences have been found in Section 2.1.

2.2.3. Step 3: Cross-ratio check along edge direction. In Fig. 3, if edge BC is a base edge, an alternative form of cross-ratio of the four points, A, B, C, D, on the extended line of the edge can be calculated as

$$R = \frac{|AC| \cdot |BD|}{|BC| \cdot |AD|}, \tag{3}$$

which is viewpoint invariant according to Duda and Hart.[15] Let the cross-ratio associated with edge e_i^1 be denoted as R_i^1, and that associated with edge e_j^2 be denoted as R_j^2. We check if the two cross-ratios, R_i^1 and R_j^2, are equal. The time complexity for comparing the two cross-ratios is O(1). Although, for every base edge, the above cross-ratios are viewpoint invariant and should have identical values in theory, numerical errors may exist in practice due to noise. (Possible sources of noise include image distortion, quantization error of image coordinates and feature extraction error, etc.) Table 1 lists the cross-ratio values computed for the boundary edges shown in Images 1 and 2 of Fig. 1 which have passed the above two steps. Two edges, e_i^1 and e_j^2, are considered as a possible corresponding base edge pairs, if

$$|R_i^1 - R_j^2| < T_1, \tag{4}$$

for some T_1. In this paper, the k-means clustering algorithm[16] is used to determine T_1 according to the distribution of cross-ratio errors, $|R_i^1 - R_j^2|$'s, for all possible (i,j).

Table 1. Cross-ratios of the four points, similar to that shown in Fig. 3, along each of the extended lines of the boundary edges shown in Fig. 2 which pass the first two steps of the procedure for finding the object base edge correspondence

Image 1		Image 2	
Vertex pairs of boundary edges	Cross-ratios R_i^1	Vertex pairs of boundary edges	Cross-ratios R_j^2
(0,1)	2.24	(0,1)	2.27
(1,2)	2.28	(1,2)	2.30
(2,3)	2.20	(2,3)	2.24
(3,4)	2.35	(3,4)	2.34
(4,5)	1.83	(5,10)	1.40
(5,10)	1.42	(10,9)	1.26
(10,9)	1.27		

2.2.4. Step 4: Cross-ratio checks for subpolygon's vertices. Since the division of the C-plate by the line containing e_i^1 is identical to that due to e_j^2 if the two edges correspond to the same object base edge, the cross-ratios of the corresponding vertices of the associated subpolygons of e_i^1 and e_j^2 are compared in this step to see if they possess the viewpoint invariant property. Because it is assumed that the C-plate contains at least five edges, in general, the two associated subpolygons of any one boundary edge will have four and five edges, respectively. (The discussion for the cases when a boundary edge is collinear with one or two C-plate vertices and that the two associated subpolygons contain less than or equal to four edges, are omitted for brevity.) In the following calculation of cross-ratios, only the associated subpolygons of e_i^1 and e_j^2 which have five edges (e.g. the subpolygons of edge BC which have vertices 21, 22, and 23 in Fig. 3) are considered.

Similar to the discussion presented in Section 2.1, Lei's cross-ratio formula [equation (1)] can be used to compute the cross-ratios of each vertex of the associated subpolygons of an object edge under consideration. Since

the vertex correspondence of the two associated subpolygons is known from step 2, it is not necessary to cyclically match the calculated cross-ratio sequences as in equation (2). Instead, the two vertex cross-ratio sequences R^1 and R^2 ($R^k = \{R_q^k \mid k = 1,2;\ q = 1,2,\ldots, U\}$) are compared to see if the sum of the squared cross-ratio differences (SCRDs) satisfies

$$\sum_{q=1}^{U} |R_q^1 - R_q^2|^2 < T_2 \tag{5}$$

for some small T_2, where R_q^k is the cross-ratio of the qth vertex of the associated subpolygon in Image k, and U is the total number of vertices of the subpolygon. In the presented experimental results, T_2 is heuristically chosen as three times the mean value of the SCRDs which have identical location of the most significant digit as that of the smallest SCRD. The time complexity of matching the two cross-ratio sequences of the two associated subpolygons is O(1). If equation (5) is not true, the proposed approach precludes the possibility that the two edges form a corresponding base edge pair.

Table 2 shows possible base vertex/edge correspondences in the two images shown in Fig. 1, in which a pair of vertices is used to represent each of the object edges. For each pair of edges, one from each image, the number of steps passed in the above four-step procedure for determining possible object base edge correspondence is indicated. For example, a "3" means the two edges pass all steps except step 4. The pairs of edges marked with a "4" correspond to most likely base edge correspondences.

Although the cross-ratio computed from Lei's formula gives some reasonable results in the above example, equation (1) is sensitive to the variation of θ_i's in Fig. 3 for small θ_2. The reason can be seen by observing the effect of the errors in θ_1, θ_2, and θ_3 on the error of cross-ratio R, respectively. Let δR, $\delta\theta_1$, $\delta\theta_2$, and $\delta\theta_3$ be the errors of R, θ_1, θ_2, and θ_3, respectively. We have

$$\delta R = \frac{\partial R}{\partial \theta_1}\delta\theta_1 + \frac{\partial R}{\partial \theta_2}\delta\theta_2 + \frac{\partial R}{\partial \theta_3}\delta\theta_3,$$

where

$$\frac{\partial R}{\partial \theta_1} = \frac{[\cos(\theta_1+\theta_2)\sin(\theta_1+\theta_2+\theta_3) - \cos(\theta_1+\theta_2+\theta_3)\sin(\theta_1+\theta_2)]\sin(\theta_2+\theta_3)}{\sin(\theta_2)\sin^2(\theta_1+\theta_2+\theta_3)}.$$

$$\frac{\partial R}{\partial \theta_2} = \frac{1}{\sin^2(\theta_2)\sin^2(\theta_1+\theta_2+\theta_3)} \times \{[\cos(\theta_1+\theta_2)\sin(\theta_2+\theta_3) + \cos(\theta_2+\theta_3)\sin(\theta_1+\theta_2)]\sin\theta_2\sin(\theta_1+\theta_2+\theta_3) - [\cos(\theta_2)\sin(\theta_1+\theta_2+\theta_3) + \cos(\theta_1+\theta_2+\theta_3)\sin(\theta_2)]\sin(\theta_1+\theta_2)\sin(\theta_2+\theta_3)\},$$

and

$$\frac{\partial R}{\partial \theta_3} = \frac{[\cos(\theta_2+\theta_3)\sin(\theta_1+\theta_2+\theta_3) - \cos(\theta_1+\theta_2+\theta_3)\sin(\theta_2+\theta_3)]\sin(\theta_1+\theta_2)}{\sin(\theta_2)\sin^2(\theta_1+\theta_2+\theta_3)}.$$

When $0° < \theta_2 < 90°$, a small θ_2 will result in a large value of $\partial R/\partial\theta_i$, because of the $\sin(\theta_2)$ term in the denominator of $\partial R/\partial\theta_i$ in the above equations. For example, the associated subpolygon of edge (0,1) in Image 1 (and in Image 2) shown in Fig. 3 has two very short edges, (51, 23) and (21, 50). Vertex 21 of the associated subpolygon of edge (0, 1) in Image 1 (2) has θ_2=10.57 (11.8) and vertex 23 in Image 1 (2) has θ_2=4.8 (7.73). Table 3 shows the cross-ratios calculated for the vertices of the associated subpolygons of edge (0,1) in the two images. Since the two cross-ratios, as well as the SCRD, calculated for vertex 21 are large (similar result can be found for vertex 23), the total

Table 2. The number of steps passed in the four-step procedure for finding the object base edge correspondence for boundary edges shown in Fig. 2*

	Boundary edge in Image 2							
Boundary edge in Image 1	(0,1)	(1,2)	(2,3)	(3,4)	(4,5)	(5,10)	(10,9)	(9,0)
(0,1)	3	1	2	1	1			1
(1,2)	1	3	1	3	1			1
(2,3)	2	1	4	1	1			1
(3,4)	1	3	1	4	1			1
(4,5)	1	2	1	2	1			1
(5,10)						4	1	
(10,9)						1	3	
(9,0)	1	1	1	1	1			1

*In step 4, the cross-ratios are computed using Lei's cross-ratio formula [equation (1)].

Table 3. Cross-ratios* of vertices of the pentagonal subpolygon of edge (0,1) shown in Image 1 and Image 2 of Fig. 2, and the sum of the squared differences of the corresponding cross ratios

Edge (0,1) in image 1		Edge (0,1) in image 2			
Vertex # of an associated subpolygon	Cross-ratios R_q^1	Vertex # of an associated subpolygon	Cross-ratio R_q^2	Absolute difference of cross-ratios $\lvert R_q^1 - R_q^2 \rvert$	$\lvert R_q^1 - R_q^2 \rvert$
50	1.21	50	1.16	0.05	0.00
51	1.22	51	1.28	0.06	0.00
23	4.56	23	3.91	0.66	0.43
22	1.04	22	1.05	0.00	0.00
21	4.73	21	5.79	1.06	1.13
Sum					1.56

*The cross-ratios are computed using Lei's cross-ratio formula.

SCRD is equal to 1.56 and the two corresponding base edges do not pass the cross-ratio check in step 4. Similar result can be shown for edge (1,2). In fact, there are examples for which the cross-ratio check yields erroneous results, i.e. the smallest total SCRD does not correspond to a correct base edge correspondence.

In order to avoid the above undesirable numerical problems due to very short edges of the associated subpolygons, different ways to compute the cross-ratios are considered in this paper. Barrett *et al.*[17] have shown that if no three of five coplanar points are collinear, the cross-ratio of one of the points can be calculated as

$$R^* = \frac{\sin\theta_2 \sin\theta_4}{\sin(\theta_1 + \theta_2)\sin(\theta_2 + \theta_3)}, \qquad (6)$$

where θ_1, θ_2, and θ_3 are defined similar to that shown in Fig. 4 and $\theta_4 = 360° - \sum_{i=1}^{3} \theta_i$. Since equation (6) is the negative reciprocal of equation (1), the cross-ratio R^* also possesses the viewpoint invariant property. Since equation (6) does not have the aforementioned numerical problem for a small θ_2, it is used in the rest of this paper for the cross-ratio check in step 4. Table 4 shows the results similar to that shown in Table 2 by using equation (6) in place of equation (1). Each of the boundary edge pairs passing all four steps corresponds to a correct base edge correspondence. Among these corresponding base edge pairs, the one with the minimum total SCRD will be used to determine the correspondence of all other object edges, as discussed next.

3. DETERMINATION OF OTHER VERTEX/EDGE CORRESPONDENCES

3.1. General procedure

Once the corresponding object base edge pair is found with the above procedure, the result is used to find the correspondences of other edges in the two images. Since each of the pair of the corresponding base edges belongs to only one object face in the individual image, the two faces can be matched using their edge sequences arranged in the clockwise (or counterclockwise) order. The matching of the two faces is considered successful if the following two conditions hold: (a) the lengths of the two edge sequences are equal and (b) the newly matched pairs of edges do not conflict with any existing matched edge pairs. After a successful matching of two faces, the two faces are marked "matched" and all the newly matched pairs of edges are recorded and attached to the end of the "matched edge pair (MEP)" queue. The above procedure continues for the next matched edge pair in the MEP queue to check whether the two edges belong to two

Table 4. The number of steps passed in the four-step procedure for finding the object base edge correspondence for boundary edges shown in Fig. 2*

	Boundary edge in Image 2							
Boundary edge in Image 1	(0,1)	(1,2)	(2,3)	(3,4)	(4,5)	(5,10)	(10,9)	(9,0)
(0,1)	3	1	2	1	1			1
(1,2)	1	4	1	3	1			1
(2,3)	2	1	4	1	1			1
(3,4)	1	3	1	4	1			1
(4,5)	1	2	1	2	1			1
(5,10)						3	1	
(10,9)						1	3	
(9,0)	1	1	1	1	1			1

*In step 4, the cross-ratios are computed using Barrett's cross-ratio formula [equation (6)].

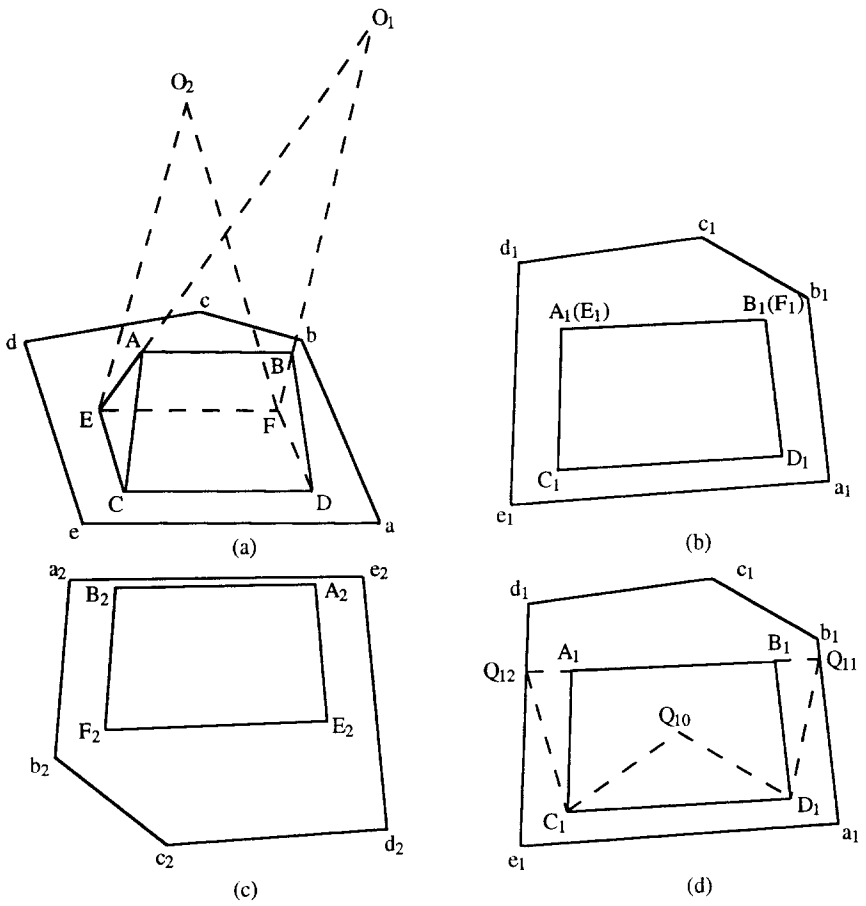

Fig. 5. (a) A tent-shaped polyhedron placed on the C-plate and two viewpoints O_1 and O_2. (b) [(c)] Perspective image of the object obtained from O_1 [O_2]. (d) A pentagon $C_1Q_{10}D_1Q_{11}Q_{12}$ constructed from face $B_1A_1C_1D_1$.

object faces which satisfy the above two conditions but have not yet been matched. The process for determining the vertex/edge correspondence is completed when the MEP queue is empty.

For the example shown in Fig. 1, the correspondences of all the object edges in the two images can be found correctly with the above procedure. The proposed procedure also works well for a partially occluded object (examples are presented in Section 5). However, there are rare occasions which occur at specific viewpoints for some special object shapes that additional procedures are required to ensure meaningful results in the correspondence, as discussed next.

3.2. *Additional procedure for special cases*

Although it is practically impossible, the conflict check in the above procedure will fail under some special circumstances. Figure 5(a) shows a tent-shaped polyhedron placed on the C-plate and two viewpoints for which the above matching process will generate erroneous results. Assume viewpoint O_1 is located at the intersection of extended lines of edges AE and BF that edges AB and EF coincide in the image; and only face $ACDB$ can be seen, as shown in Fig. 5(b). If viewpoint O_2 is located at the other side of the object from which only face $AEFB$ can be seen, as shown in Fig. 5(c), according to the base vertex/edge correspondence finding procedure presented in Section 2, edge B_1A_1 in Image 1 and edge F_2E_2 in Image 2 will form a matched base edge pair. Furthermore, the other edges of the two faces $B_1A_1C_1D_1$ and $F_2E_2A_2B_2$ will be matched successfully, according to the above general procedure.

If viewpoint O_2 is located such that AB and CD do not coincide in the image, faces $BACD$ and $FEAB$ do not correspond to perspective projections of the same planar object onto the C-plate. Therefore, a viewpoint invariant measure such as the cross-ratio can be used to prevent an establishment of correspondence between them. Since the cross-ratio can only be calculated for the vertices of a polygon which has at least five vertices, and no three of them are collinear, the polygon with the following five vertices is used instead: the two intersection points of the extended line of the base edge and the C-plate boundary, the two vertices which do not belong to the base edge, and the intersection point of the two diagonals of the face. Figure 5(d) shows the pentagon constructed from face $B_1A_1C_1D_1$. Using the cross-ratio check similar to that

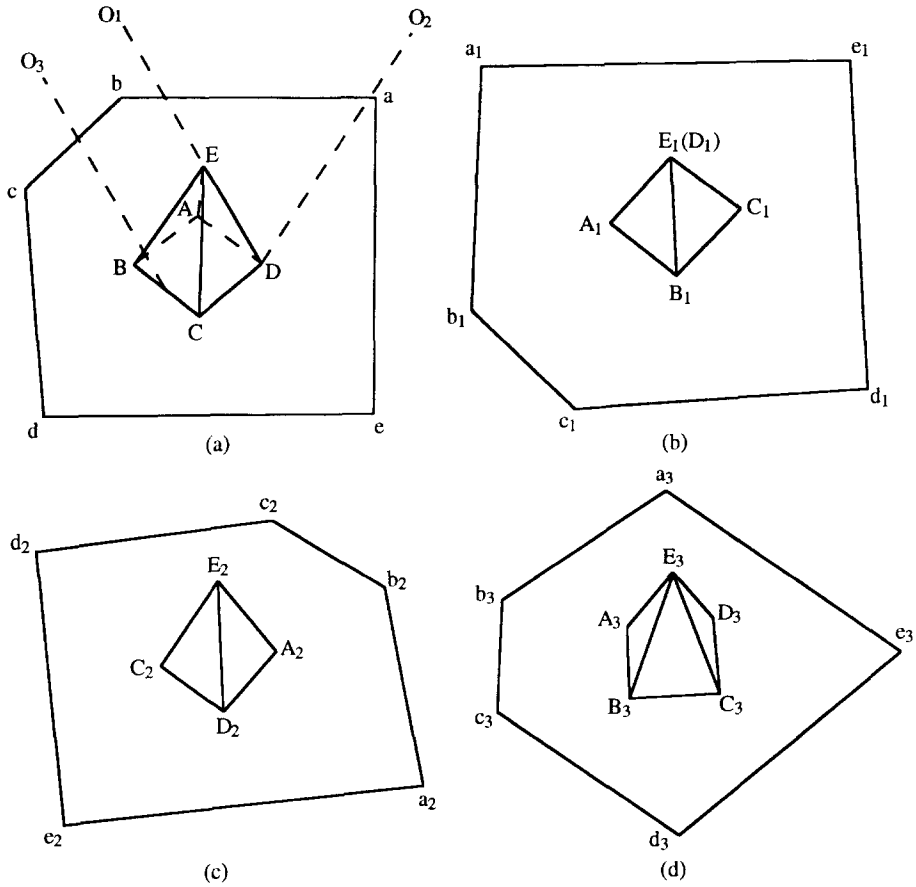

Fig. 6. Perspective image of (a) A pyramid placed on the C-plate and three viewpoints O_1, O_2 and O_3. (b) The object image obtained from O_1. (c) The object image obtained from O_2. (d) The object image obtained from O_3.

described in Section 2.2.4, the two newly constructed pentagons, and thus the two faces $B_1A_1C_1D_1$ and $F_2E_2A_2B_2$, will not result in a match.

On the other hand, in an extremely rare situation, if viewpoint O_2 is located at the intersection of extended lines of edges AC and BD with the location of O_1 unchanged, edges AB and CD will coincide in the image that C_1D_1 and A_2B_2 will also form a matched base edge pair. With the above information alone, the only conclusion one can make is that the two faces match perfectly and the corresponding object is a polygon which is coplanar with the C-plate, i.e. the ambiguity problem is not resolvable in 2-D space. (However, the ambiguity can be detected in 3-D space.)

As another example of a special case, Fig. 6 shows the pyramid-shaped object that each visible object face contains only three vertices. Assume viewpoint O_1 is located at the extended line of edge DE so that edges EC and DC coincide in the image (and so do edges EA and DA), and only faces ABE and BCE can be seen. If viewpoint O_2 is located at the other side of the object from which only faces CDE and ADE can be seen, according to the base vertex/edge correspondence finding procedure presented in Section 2, edge E_1A_1 in Image 1 and edge D_2A_2 in Image 2 will form a matched base edge pair, and so do edges C_1E_1 and C_2D_2. Furthermore, the other edges of the two faces $E_1A_1B_1$ and $D_2A_2E_2$ will be matched successfully, and so do those of the two faces $C_1E_1B_1$ and $C_2D_2E_2$, according to the general procedure presented in this section. Due to the special object geometry, a procedure similar to that developed for Fig. 5 to construct polygons of more than four vertices from object faces has not been found. Additional information can be introduced to resolve the ambiguity problem. For example, if a third viewpoint O_3 is located near O_1 as shown in Fig. 6(a), and can see three faces, ABE, BCE, and CDE, edge A_1B_1 in Image 1 and edge A_3B_3 in Image 3 will form a matched base edge pair (so do edges B_1C_1, and B_3C_3, and edges C_1E_1 and C_3D_3). However, according to the procedure presented in Section 3.1, we can detect conflicts in the object geometry except for the first base edge pair which corresponds to a correct match.

4. DETERMINATION OF OBJECT VERTEX/EDGE CORRESPONDENCES WITH PARTIALLY OCCLUDED C-PLATE BOUNDARY

The proposed approach can be extended to situations when the C-plate boundary is partially occluded as long

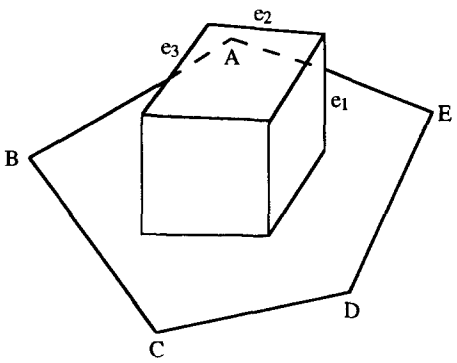

Fig. 7. An example of a partially occluded C-plate.

as the complete boundary can be recovered. For example, if the visible part of each of the C-plate edges is of finite length (see Fig. 7), the complete C-plate boundary can be reconstructed through simple interpolation. In this case, if it is known *a priori* that the base face of the object is internal to the C-plate boundary, the object boundary edges which are not completely inside the C-plate boundary can be ruled out in the base edge correspondence check.

5. EXPERIMENTAL RESULTS

In this section, experimental results for the determination of vertex/edge correspondences for an object in two images are presented. For an object placed on the C-plate, two images are taken from two different viewing angles, denoted as Images 1 and 2 of the object, respectively. The objects used in the experiments include two polyhedra and two curved objects. Figures 8–11 show the images of these objects. While edges of polyhedra are marked with dark lines, dark grid lines are pasted on the surface of the curved objects.

Once images of an object are obtained, line features are extracted for the object as well as the C-plate. Figures 12 and 13 show the extracted features for Figs 8 and 9, respectively, with the object vertices marked with identification numbers. Tables 5 and 6 show the results of the base edge correspondence finding procedure, similar to Table 4, for object boundary edges shown in Figs 12 and 13, respectively. Figures 14 and 15 show the corresponding edges obtained by the proposed approach for Figs 8 and 9, respectively. Tables 7 and 8 show the results of the base edge correspondence finding procedure for selected edges shown in Figs 16 and 17, respectively, for the curved objects. One can verify that the base edge corre-

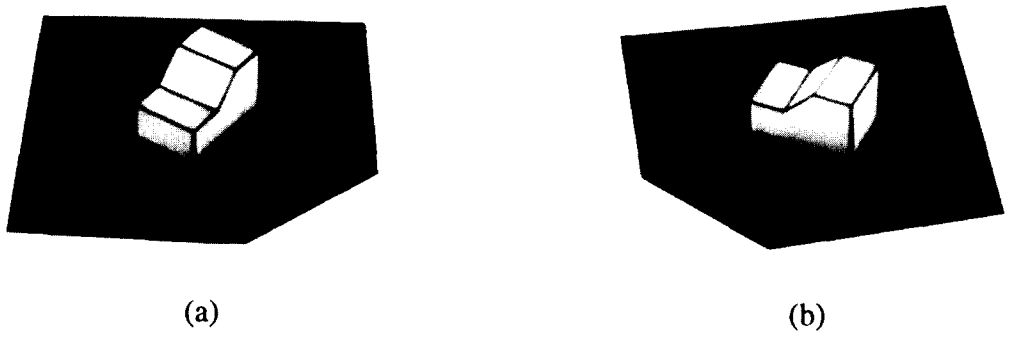

Fig. 8. Two views of a polyhedron placed on the C-plate. (a) Image 1. (b) Image 2.

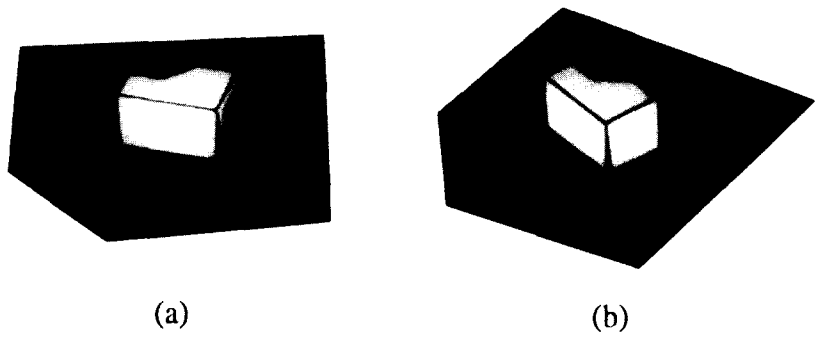

Fig. 9. Two views of the polyhedron shown in Fig. 8 but placed differently on the C-plate. (a) Image 1. (b) Image 2.

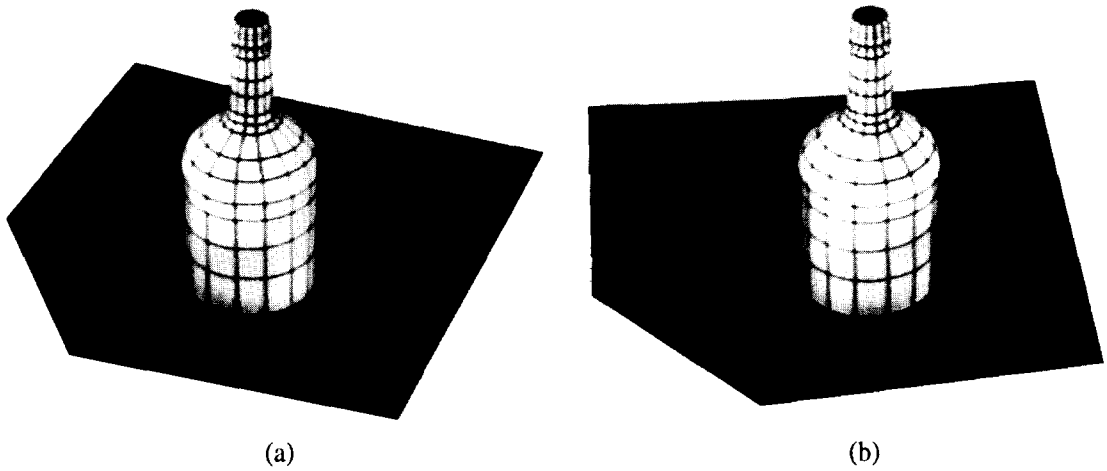

(a) (b)

Fig. 10. Two views of a bottle-shaped object placed on the C-plate. (a) Image 1. (b) Image 2.

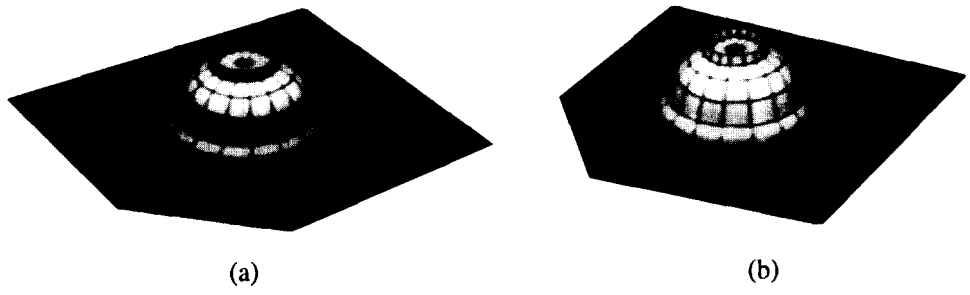

(a) (b)

Fig. 11. Two views of a bowl-shaped object placed on the C-plate. (a) Image 1. (b) Image 2.

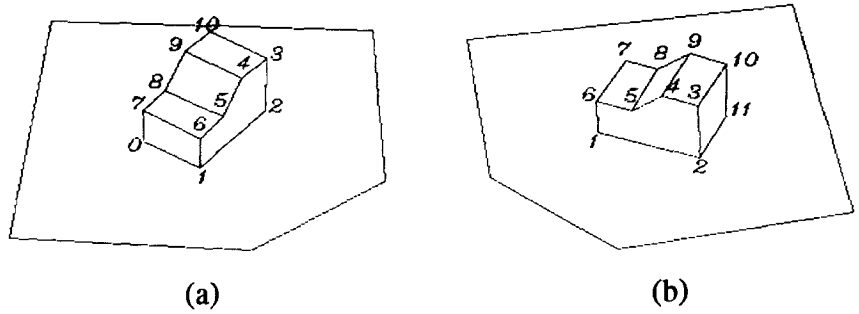

(a) (b)

Fig. 12. Edges extracted from (a) Image 1 and (b) Image 2 of Fig. 8.

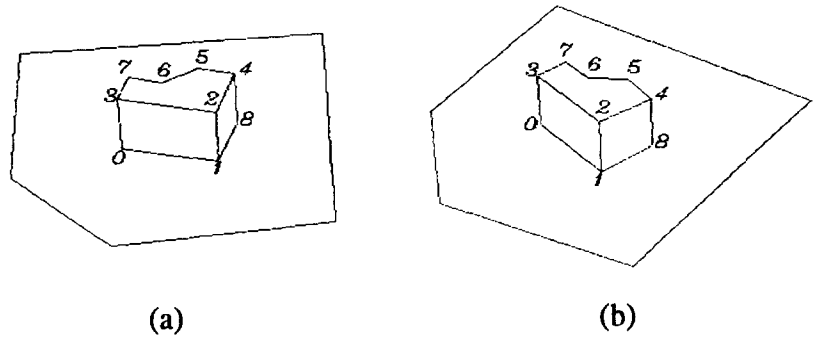

(a) (b)

Fig. 13. Edges extracted from (a) Image 1 and (b) Image 2 of Fig. 9.

Table 5. The number of steps passed in the four-step procedure for finding the object base edge correspondence for boundary edges shown in Fig. 12

	Boundary edge in Image 2							
Boundary edge in Image 1	(1,2)	(2,11)	(11,10)	(10,9)	(9,8)	(8,7)	(7,6)	(6,1)
(0,1)		1	1	1	1	1	3	
(1,2)	4							1
(2,3)	1							1
(3,10)		2	1	1	1	1	1	
(10,9)		1	1	2	1	2	1	
(9,8)		1	1	1	1	1	1	
(8,7)		1	1	2	1	3	1	
(7,0)		1	1	1	1	1		

Table 6. The number of steps passed in the four-step procedure for finding the object base edge correspondence for boundary edges shown in Fig. 13

	Boundary edge in Image 2							
Boundary edge in Image 1	(0,1)	(1,8)	(8,4)	(4,5)	(5,6)	(6,7)	(7,3)	(3,0)
(0,1)	4	1	1					1
(1,8)	1	3	1					1
(8,4)	1	2	1					1
(4,5)				1	1	1	1	
(5,6)				1	3	1	1	
(6,7)				2	1	2	1	
(7,3)				1	1	1	2	
(3,0)	1	1	1					1

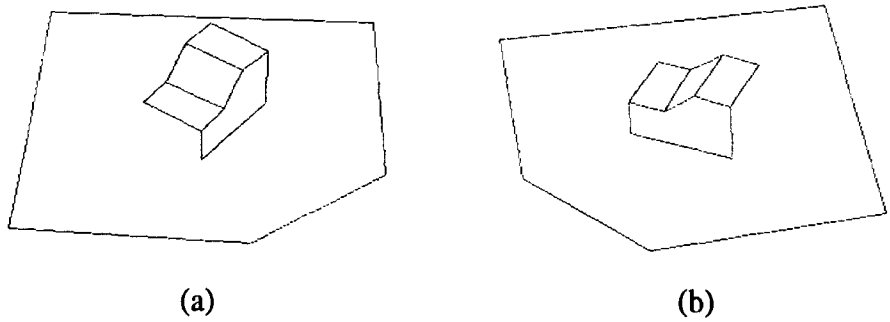

Fig. 14. Edges in (a) Image 1 and (b) Image 2 of Fig. 12 for which the vertex/edge correspondences have been established.

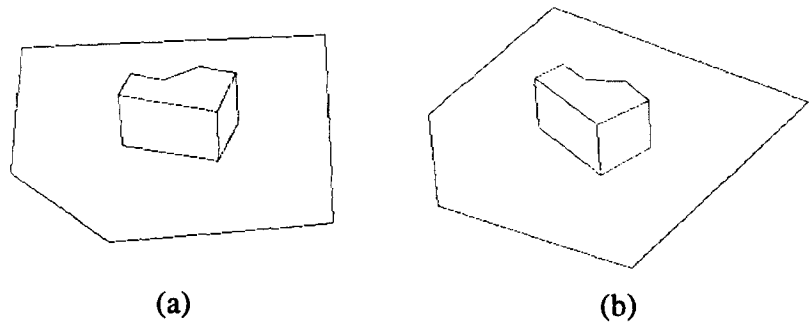

Fig. 15. Edges in (a) Image 1 and (b) Image 2 of Fig. 13 for which the vertex/edge correspondences have been established.

Table 7. The number of steps passed in the four-step procedure for finding the object base edge correspondence for some selected boundary edges shown in Fig. 16

Boundary edge in Image 1	Boundary edge in Image 2			
	(0,1)	(1,2)	(2,3)	(3,4)
(0,1)	2	2	1	1
(1,2)	1	1	3	3
(2,3)	1	1	3	4
(3,4)	1	1	1	1
(4,5)	1	1	1	1

Table 8. The number of steps passed in the four-step procedure for finding the object base edge correspondence for some selected boundary edges shown in Fig. 17

Boundary edge in Image 1	Boundary edge in Image 2				
	(0,1)	(1,2)	(2,3)	(3,4)	(4,5)
(0,1)	1	1	1	1	1
(1,2)	1	1	1	1	1
(2,3)	1	1	1	1	1
(3,4)	2	1	1	1	1
(4,5)	1	4	2	1	1

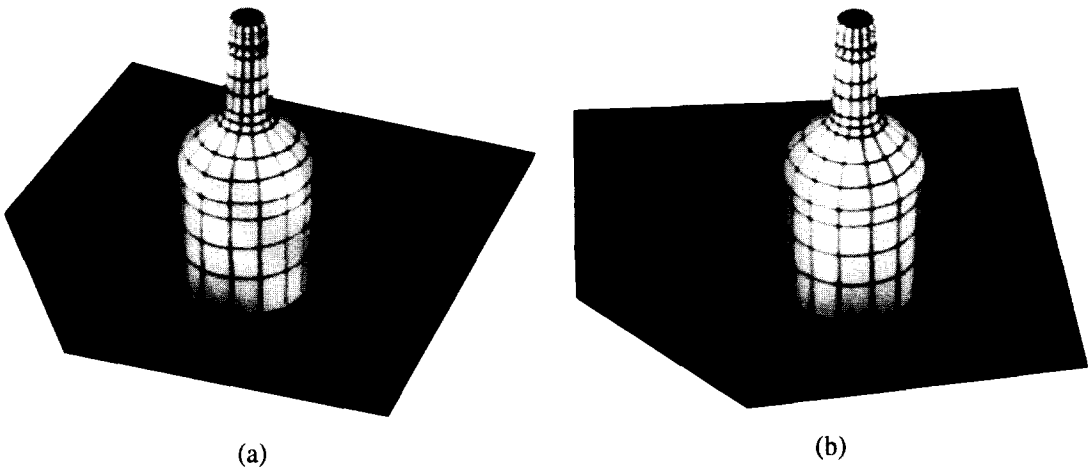

Fig. 16. The two views of the bottle-shaped object placed on the C-plate with identification numbers marked for some vertices. (a) Image 1. (b) Image 2.

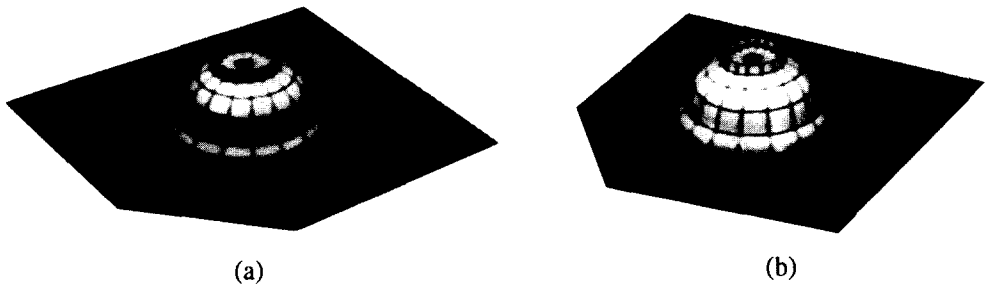

Fig. 17. The two views of the bowl-shaped object placed on the C-plate with identification numbers marked for some vertices. (a) Image 1. (b) Image 2.

spondence for each of the curved objects is correct. The other corresponding edges similar to that shown in Fig. 14 can also be derived for the curved object. The results are not shown for brevity.

6. CONCLUSION

In this paper, we have presented a novel approach which uses the extra information provided by a calibration polygon, the C-plate, to solve the object vertex/edge correspondence problem. We first determine the C-plate vertex correspondence in two images by comparing the cross-ratios of C-plate vertices. The result is then used to simplify the subsequent procedure for finding the object base vertex/edge correspondence. Only object boundary edges in the two images need to be considered for possible base edge correspondence. Simple geometric relations with other features in the image as well as

viewpoint invariant properties associated with a base edge are examined in finding the correspondence. The former are concerned with (i) the object face containing the edge and (ii) the subpolygons obtained by dividing the C-plate with the extended line of the edge. The latter, on the other hand, involve the calculation of the viewpoint invariant measure, e.g., cross-ratio, for (i) relative location of the edge in the C-plate along the direction of the edge, and (ii) the associated subpolygons. Once the object base edge correspondence has been determined, the correspondence of other edges can be determined in a straightforward manner using one of the corresponding base edge pairs, except for some very special situations. The special situations are involved with images acquired at specific viewpoints for some special object shapes, and may result in ambiguity in the correspondence. An additional procedure may be carried out to resolve the problem and is briefly discussed.

The proposed approach has several advantages compared with other approaches for solving similar problems. First, it uses only 2-D image data and does not require 3-D information, so it is simple and efficient. Second, unlike Lei's method, the number of vertices of an object face can be less than five. Third, with the predetermined vertex correspondence of the C-plate, the search space for finding base vertex/edge correspondence is greatly reduced. Finally, the ambiguity in the correspondence can be resolved for general situations.

An important usage of the calibration polygon was given in Chiu *et al.*,[18] where the calibration polygon is used for camera calibration in an on-line fashion, so that a single camera can be moved around to take stereo images from a fairly large range of viewing angles for 3-D reconstruction. Since the two images can be taken with nearly orthogonal optical axes, we can generally obtain the results which are less sensitive to the feature point position errors for a triangulation process and, therefore, are more accurate than those obtained by the conventional stereo vision methods.

Theoretically, the use of the calibration polygon, the C-plate, in this paper is, in some sense, equivalent to assuming the known shape of a visible polygonal face of a polyhedron. With this augmented calibration plate which is under our control, we can determine the feature correspondences in a pair of stereo images for a fairly general object which has at least a visible base edge (real or virtual) on the calibration plate.

REFERENCES

1. S. T. Barnard and M. A. Fischler, Computational stereo, *Comput. Surveys* **14**(4), 553–572 (1982).
2. U. R. Dhond and J. K. Aggarwal, Structure from stereo—A review, *IEEE Trans. Systems Man Cybernet.* **19**(6), 1489–1510 (1989).
3. M. C. Leu and R. M. Pherwani, Vision system for three-dimensional position measurement based on stereo disparity, *Optics Laser Tech.* **21**(5), 319–324 (1989).
4. X. W. Tu and B. Dubuisson, 3-D information derivation from a pair of binocular images, *Pattern Recognition* **23**(3/4), 223–235 (1990).
5. M. Herman and T. Kanade, Incremental reconstruction of 3-D scenes from multiple, complex images, *Artificial Intelligence* **30**(3), 289–341 (1986).
6. K. C. Hung, R. N. Chiou, C. N. Shyi, J. Y. Lee and C. H. Chen, Polyhedron reconstruction using three-view analysis, *Pattern Recognition* **22**(3), 231–246 (1989).
7. R. Horaud and T. Skordas, Stereo correspondence through feature grouping and maximal cliques, *IEEE Trans. Pattern Analysis Mach. Intell.* **11**(11), 1168–1180 (1989).
8. N. Ayache and F. Lustman, Trinocular stereo vision for robotics, *IEEE Trans. Pattern Analysis Mach. Intell.* **13**(1), 73–85 (1991).
9. S. H. Lee and J. J. Leou, A dynamic programming approach to line segment matching in stereo vision, *Pattern Recognition* **27**(8), 961–986 (1994).
10. M. Ito and A. Ishii, Three-view stereo analysis, *IEEE Trans. Pattern Analysis Mach. Intell.* **PAMI-8**, 524–532 (1986).
11. M. T. Boraie and M. A. Sid-Ahmed, Points of correspondence in stereo images with no specific geometrical constraints using mathematical morphology, *Computers In Industry* **20**, 295–310 (1992).
12. D. Yang and J. Illingworth, Line based trinocular stereo, *Proc. British Machine Vision Conf.*, University of Leeds, pp. 327–336 (1992).
13. E. Grosso, G. Sandini and M. Tistarelli, 3-D object reconstruction using stereo and motion, *IEEE Trans. Systems Man Cybernet.* **19**(6), 1465–1476 (1989).
14. G. Lei, Recognition of planar objects in 3-D space from single perspective views using cross-ratio, *IEEE Trans. Robotics Automat.* **6**(4), 432–437 (1990).
15. R. O. Duda and P. E. Hart, *Pattern Classification and Scene Analysis*. Wiley, New York (1973).
16. J. MacQueen, Some methods for classification and analysis of multivariate observations, *Proc. Fifth Berkely Symp. Math. Statist. Prob.*, L. Le Cam and J. Neyman, eds, vol. **1**, pp. 281–297 (1967).
17. E. B. Barrett, P. M. Payton, N. N. Haag and M. H. Brill, General methods for determining projective invariants in imagery, *CVGIP: Image Understanding* **53**(1), 46–65 (1991).
18. J. M. Chiu, Z. Chen and C. M. Wang, 3-D polyhedral face computation from two perspective views with the aid of a calibration plate, *IEEE Trans. Robotics Automat.* (to appear).

About the Author—JUI-MAN CHIU received the B.S. degree in Statistics from Fu Jen Catholic University, Taipei, Taiwan, R.O.C., in 1982, and the M.S. degree in Statistics from National Chengchi University, Taipei, Taiwan, R.O.C., in 1984. From 1984 to 1992, she was an Assistant Research Engineer at Network Planning Laboratory, Telecommunication Laboratories, Ministry of Transportation and Communications, Taiwan, R.O.C. From 1985 to 1987, she was also a lecturer with Fu Jen Catholic University. She is currently a Ph.D. candidate in the Institute of Computer Science and Information Engineering at National Chiao Tung University, Hsinchu, Taiwan, R.O.C. Her research interests include computer vision, image processing, pattern recognition and telecommunication networks. She is a member of the Chinese Society for Image Processing and Pattern Recognition.

About the Author—ZEN CHEN received the B.Sc. degree from National Taiwan University, Taiwan, R.O.C., in 1967, the M.Sc. degree from Duke University, Durham, North Carolina, U.S.A., in 1970, and the Ph.D. degree

from Purdue University, West Lafayette, Indiana, in 1973, all in Electrical Engineering. From 1973 to 1974, he was with Burroughs Corporation, Detroit, Michigan, where he was engaged in the development of a document recognition system. Since 1974, he has been on the faculty of National Chiao Tung University, Taiwan, R.O.C. He served as the Director of the Institute of Computer Engineering from 1975 to 1980. He spent his sabbatical leave at Lawrence Berkeley Lab., University of California, Berkeley, CA, during 1981–1982, and, later, at the Center for Automation Research, University of Maryland, College Park, MD, in 1989. His current research interests include computer vision, CAD/CAM systems, pattern recognition and parallel algorithms and architectures. Dr Chen is a member of Sigma Xi and Phi Kappa Phi. He is also a member of China Computer Society, the Chinese Institute of Electrical Engineering and the Chinese Society for Image Processing and Pattern Recognition.

About the Author — JEN-HUI CHUANG received the B.S. degree in Electrical Engineering from National Taiwan University in 1980, the M.S. degree in Electrical and Computer Engineering from the University of California at Santa Barbara in 1983, and the Ph.D. degree in Electrical and Computer Engineering from the University of Illinois at Urbana-Champaign in 1991. Between 1980 and 1982 he was a Maintenance Officer for the HAWK missile system with the Chinese Army. Between 1983 and 1985 he was a Design and Development Engineer with the LSI Logic Corporation, Milpitas, California. Between 1985 and 1989 he was a Research Assistant at the University of Illinois. Between 1989 and 1991 he was a Research Assistant with the Robot Vision Laboratory at the Beckman Institute for Advanced Science and Technology, University of Illinois. Since August 1991, he has been on the faculty of the Department of Computer and Information Science at National Chiao Tung University. His research interests include robotics, computer vision, speech and image processing and VLSI systems. Dr Chuang is a member of IEEE and the Tau Beta Pi Society.

About the Author — TSORNG-LIN CHIA received the B.S. degree in Electrical Engineering from Chung Cheng Institute of Technology, Taoyuan, Taiwan, in 1982, the M.S. and Ph.D. degrees in Computer Science and Information Engineering from National Chiao Tung University, Hsinchu, Taiwan, in 1986 and 1993, respectively. He has been on the faculty of the Chung Cheng Institute of Technology since 1982, where he is currently an Associate Professor in the Department of Electrical Engineering. His research interests include image processing, computer vision and parallel algorithms and architecture.